An Improved Equivalent Magnetic Circuit Network Method for Consideration of Motional Eddy Currents in a Solid Conductor

Hooshang Gholizad[i] ; Mojtaba Mirsalim [ii]; Mehran Mirzaei[iii]

ABSTRACT

In this paper, an improved equivalent magnetic circuit network method to model eddy currents caused by relative motion in solid conductors is presented. The proposed method can accurately model the motional eddy currents by only using magnetic circuits and the scalar potential. Comparison of the simulation results with those of the two-dimensional finite element method proves the capability of the proposed method in modeling the motional eddy currents with high accuracy.

KEYWORDS

Motional Eddy Current, Solid Conductor, Equivalent Magnetic circuit Network

1. INTRODUCTION

Modeling of motional eddy current is very important in electromagnetic devices such as solid-rotor motors, high-speed induction motors, and dc brakes. The Magnetic Equivalent Circuit (MEC) method is one of the oldest methods in modeling magnetic devices with conducting regions. It is conventionally based on Ohm's and Kirchhoff's laws for magnetic and electric circuits [1]-[3].

Several papers about the implementation of MEC to eddy current modeling have been presented in the literature [2]-[6]. But, none can analyze the exact effect of the motional eddy current in a conduction sheet. The reason is that, they have all modeled eddy current effects approximately by using an electric circuit. In some problems such as conducting plates, due to unpredictable current distribution, the construction of electric circuits is inaccurate if not impossible.

Hur [7]-[9] has developed the Equivalent Magnetic Circuit Network (EMCN) method which uses a single network that includes both magnetic and electric fields. It not only replaces vector quantities by a scalar one but also takes into account the eddy currents. It can easily analyze the eddy current in a conduction sheet with less computation time than other 3-D numerical techniques. But, Hur's development only modeled the stationary eddy currents.

In this paper, a new formulation for modeling motional eddy current problems using only magnetic circuits is presented. The theory can also be extended to 3-D problems. By the combination of the proposed method with the one presented in [8] and [9], the equivalent magnetic circuit network method will be able to solve the electromagnetic problems by only using the magnetic scalar potential, as precisely as the finite element method (FEM). Therefore, the proposed method particularly in three dimensional cases will take shorter time and require less memory because of using only one variable for each node (magnetic scalar potential of the node) instead of three variables required in the FEM.

To prove the capability and the accuracy of the method in modeling the motional eddy currents, an electromagnetic brake with linear motion is simulated, and then, the EMCN results are compared with the 2-D finite element model. It will be shown that the proposed EMCN method can model the motional eddy currents with high accuracy.

2. MODELING OF MOTIONAL EDDY CURRENT

This approach is achieved by taking into account the motional eddy current in the Equivalent Magnetic Circuit Network method formulation. Figure 1 shows a schematic of the analyzed electromagnetic brake. As it is shown in Figures 2 and 3, the electromagnetic brake model is divided into rectangular elements and then, an equivalent magnetic circuit network is constructed by connecting the

[i]H. Gholizad is with the Department of Electrical Engineering, Amirkabir University of Technology, Tehran, Iran (e-mail: Gholizad@aut.ac.ir,).
[ii] M. Mirsalim is with the Department of Electrical Engineering, Amirkabir University of Technology, Tehran, Iran (e-mail: Mirsalim@aut.ac.ir).
[iii] M. Mirzayee is with the Electrical Machines & Transformers Research Laboratory (EMTRL), Amirkabir University of Technology, Tehran, Iran.(e-mail: Mehran_Mirzayee@yahoo.com)

center of neighboring elements. Due to the symmetry shown in Figure 2, only one half of the electromagnetic brake model is taken into account in the construction of the equivalent magnetic circuit network. Also, the value of magnetic scalar potential in the middle of the solid conductor is constant due to symmetrical construction of the model of the brake and it can be set to zero as a reference for magnetic scalar potential.

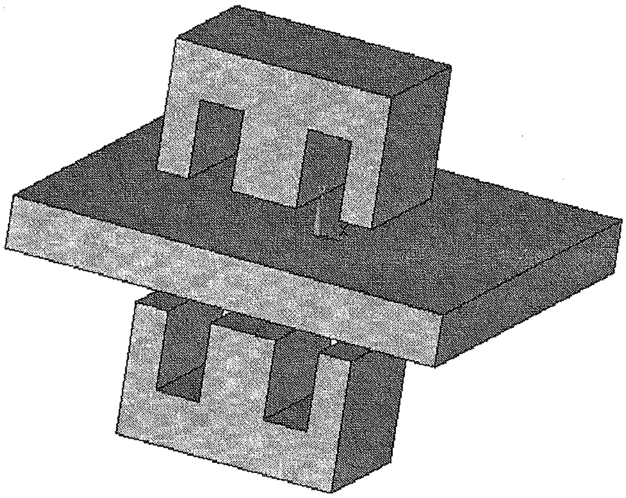

Figure 1: An electromagnetic brake.

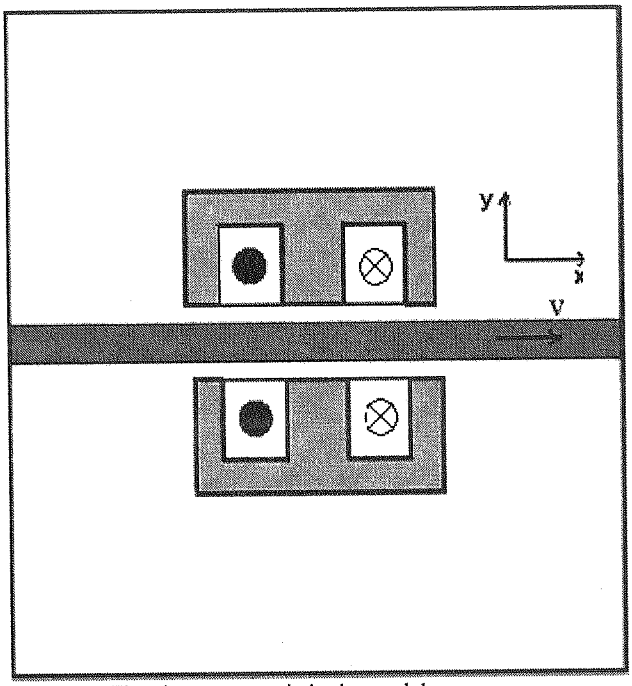

Figure 2: The electromagnetic brake model.

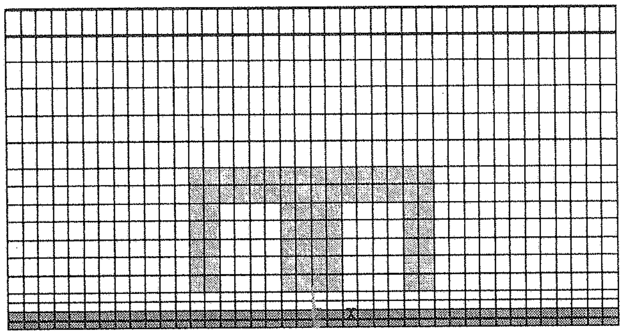

Figure 3: Rectangular elements of the model.

The effect of motional eddy current is considered by additional magnetomotive forces (MMF) in the conducting regions. The value for the MMF source should be cumulative starting from the middle to the top of the solid conductor. In fact, one should enter the MMF sources caused by the induced current of all upper elements in the conducting plate model.

To avoid the MMF sources to become accumulated to the top of the model which makes the equations complicated, two magnetic scalar potential is used; one for the solid conductor and another for the rest of the model. By using two magnetic scalar potential, the value for the MMF sources could be cumulative starting from the middle of solid conductor to the air-gap border-regions of the conductor instead of the top of the model.

The related equations to analyze the electromagnetic devices with moving parts and static sources are as follows:

$$\nabla \bullet \boldsymbol{B} = 0, \quad \nabla \times \boldsymbol{B} = \mu \boldsymbol{J}, \quad \boldsymbol{J_e} = \sigma(\boldsymbol{V} \times \boldsymbol{B}) \tag{1}$$

where, J_e is the motional eddy current density and σ, and v are the conductivity and the velocity of the moving part, respectively.

For non-conducting elements which MMF due to stator winding does not have any influence, such as air gap, an equivalent model consists of four reluctances connected to the neighboring elements at a node. The equation for the balance of fluxes of those elements shown in Figure 4 is as in the following:

$$\begin{aligned} &\frac{U_{i,j} - U_{i-1,j}}{\{R^y_{i,j} + R^y_{i-1,j}\}/2} + \frac{U_{i,j} - U_{i,j-1}}{\{R^x_{i,j} + R^x_{i,j-1}\}/2} + \\ &\frac{U_{i,j} - U_{i+1,j}}{\{R^y_{i,j} + R^y_{i+1,j}\}/2} + \frac{U_{i,j} - U_{i,j+1}}{\{R^x_{i,j} + R^x_{i,j+1}\}/2} = 0 \end{aligned} \tag{2}$$

where, $U_{i,j}$, $R^x_{i,j}$ and $R^y_{i,j}$ are the magnetic scalar potential, and the horizontal and the vertical components of the reluctance of the element denoted by *(i,j)*, respectively.

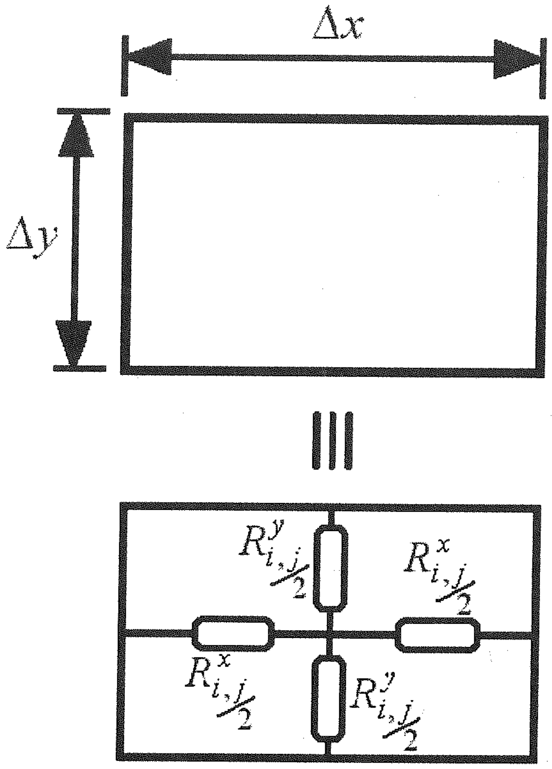

Figure 4: The model of a non-conducting rectangular element.

For a rectangular element which is shown in Figure 4 the horizontal and vertical components of the reluctance of the element can be written as below:

$$\begin{cases} R_{i,j}^{x} = \dfrac{\Delta x}{\mu L \Delta y} \\ R_{i,j}^{y} = \dfrac{\Delta y}{\mu L \Delta x} \end{cases} \tag{3}$$

where, Δx and Δy are the horizontal and vertical dimensions of the element, respectively, and L denotes the depth of the element.

For the elements in the winding region of stator, two additional MMF sources due to the currents of stator windings are used in the horizontal orientation. The equation for the balance of fluxes in the elements shown in Figure 5 is as in the following:

$$\frac{U_{i,j}-U_{i-1,j}}{\{R_{i,j}^{y}+R_{i-1,j}^{y}\}/2}+\frac{U_{i,j}-U_{i,j-1}-F_{i,j}-F_{i,j-1}}{\{R_{i,j}^{x}+R_{i,j-1}^{x}\}/2}+ \frac{U_{i,j}-U_{i+1,j}}{\{R_{i,j}^{y}+R_{i+1,j}^{y}\}/2}+\frac{U_{i,j}-U_{i,j+1}+F_{i,j}+F_{i,j+1}}{\{R_{i,j}^{x}+R_{i,j+1}^{x}\}/2}=0 \tag{4}$$

where, $F_{i,j}$ is magnetomotive force due to stator winding currents in the corresponding element. As it is shown in Figure 5, each magnetomotive force $F_{i,j}$ is equal to half of the stator current in the hatched area, i.e.

$$F_{i,j}+F_{i,j}=\Delta I \quad \Rightarrow \quad F_{i,j}=\Delta I/2 \tag{5}$$

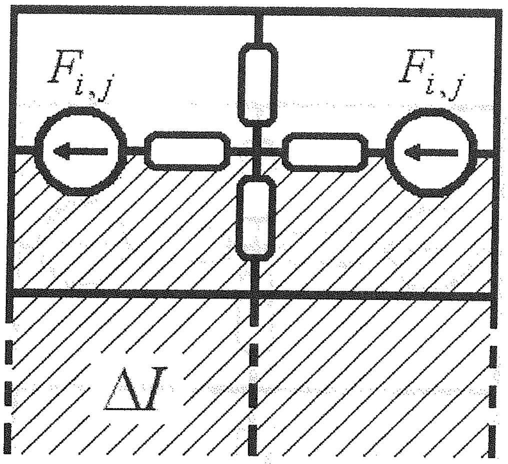

Figure 5: MMF due to stator winding currents.

Figure 6 shows a number of neighboring elements in the border regions of the air-gap. For each element in the conducting region within the rotor, two additional MMF sources due to induced currents are used in the radial orientation.

The flux balance equation for such elements which is shown in Figure 7 can be written as in the following:

$$\frac{U_{i,j}-U_{i-1,j}}{\{R_{i,j}^{y}+R_{i-1,j}^{y}\}/2}+\frac{U_{i,j}-U_{i,j-1}-F_{i,j}^{ind}-F_{i,j-1}^{ind}}{\{R_{i,j}^{x}+R_{i,j-1}^{x}\}/2}+ \frac{U_{i,j}-U_{i+1,j}}{\{R_{i,j}^{y}+R_{i+1,j}^{y}\}/2}+\frac{U_{i,j}-U_{i,j+1}+F_{i,j}^{ind}+F_{i,j+1}^{ind}}{\{R_{i,j}^{x}+R_{i,j+1}^{x}\}/2}=0 \tag{6}$$

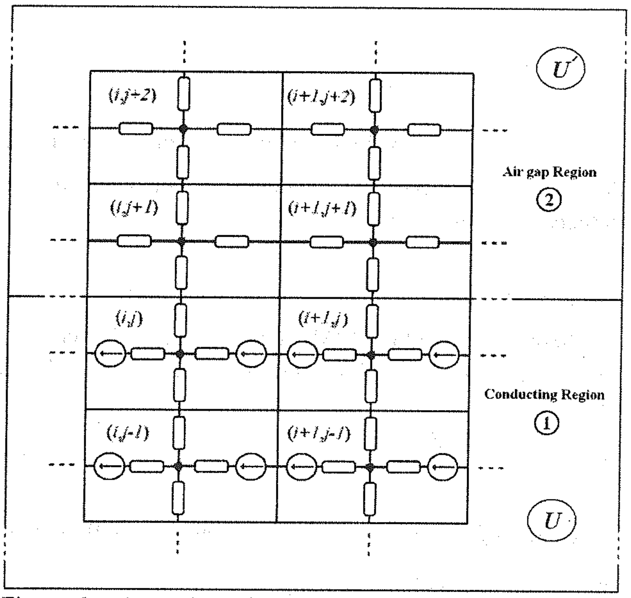

Figure 6: A number of neighboring elements in the air-gap border regions.

where, $F_{i,j}^{ind}$ is the MMF produced by the induced currents in the corresponding element. As it is shown in Figure 7, the following equation can be written between magnetomotive forces $F_{i,j}^{ind}$ and $F_{i-1,j}^{ind}$:

$$2F_{i,j}^{ind} - 2F_{i-1,j}^{ind} = \Delta I_{ind} \tag{7}$$

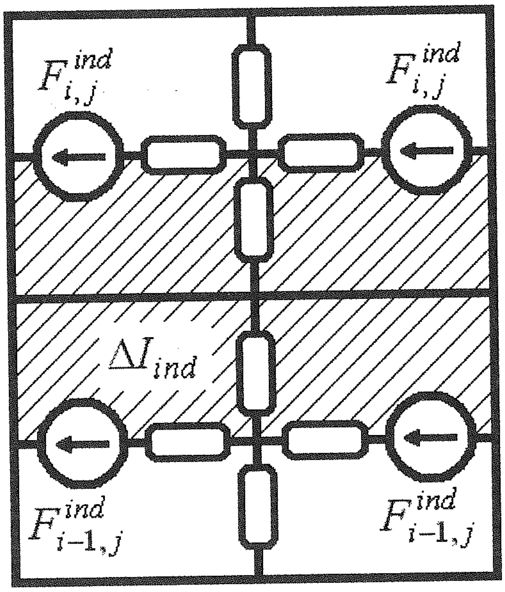

Figure 7: MMF due to induced currents in conducting elements.

For the purpose of calculation of the magnetomotive force, ($F_{i,j}^{ind}$), produced by the induced currents, the following equation can be derived from the basic equations in (1):

$$\begin{aligned} J_{ez} &= \sigma V_x B_y = \sigma V_x \left(\frac{\phi_y}{A}\right) \\ &= \mu\sigma V_x \left(\frac{U_{i,j} - U_{i-1,j}}{\Delta y}\right) \end{aligned} \tag{8}$$

where, V_x is the velocity of the moving part in the x direction. Now, according to Figure 7, the value of the induced current in the hatched area can be written as below:

$$\Delta I_{ind} = J_{ez}\Delta x \Delta y = \mu\sigma V_x \left(U_{i,j} - U_{i-1,j}\right)\Delta x \tag{9}$$

Therefore, the added MMF sources in the element *(i,j)* can be calculated by taking into account (7) and (9) as follows:

$$F_{i,j}^{ind} = \frac{\mu\sigma V_x U_{i,j}\Delta x}{2} = GU_{i,j} \tag{10}$$

where, $G = \mu\sigma V_x \Delta x/2$ is a constant coefficient in the conducting region.

Thus, it is possible to model motional eddy currents in solid conductors and to analyze the characteristics of the electromagnetic devices in two dimensions. This method could also be extended to three dimensions.

As mentioned above, two different magnetic scalar potentials are used; one for the solid conductor (U) in region 1 and another for the rest of the model (U') in region 2 including the air-gap. Boundary conditions between the two regions with different scalar potentials are as in the following:

$$\begin{cases} B_y(region\,1) = B_y(region\,2) \\ H_x(region\,1) = H_x(region\,2) \end{cases} \tag{11}$$

where, B is the magnetic flux density, H the magnetic field intensity, region 1 the area from the middle of the solid conductor to the air-gap border-regions of the conductor, and region 2 is the rest of the model.

Equation (11) in terms of scalar potentials can now be rewritten as below:

$$\begin{cases} \dfrac{\mu_r \Delta x\left(U_{i,j} - U_{i,j-1}\right)}{\Delta y} = \dfrac{\Delta x'\left(U'_{i,j+2} - U'_{i,j+1}\right)}{\Delta y'} \\ \dfrac{\Delta y\left(U_{i+1,j} - U_{i,j} + F_{i,j}^{ind} + F_{i+1,j}^{ind}\right)}{\Delta x} = \\ \dfrac{\Delta y'\left(U'_{i+1,j+1} - U'_{i,j+1}\right)}{\Delta x'} \end{cases} \tag{12}$$

where, $U_{i,j}$ and $U'_{i,j+1}$ are the magnetic scalar potentials of the node *(i,j)* in the conducting region 1, and of the node *(i,j+1)* in the air-gap within region 2, respectively. Also Δx, Δy and $\Delta x'$, $\Delta y'$ are respectively small variations for x and y directions in the conducting regions 1 and 2.

Therefore, by using two magnetic scalar potentials, the induced MMF sources can be eliminated in the air-gap and upper elements which improves the matrix sparsity patterns.

3. Simulation Results

In order to verify the effectiveness and accuracy of the proposed method, the simulation results for flux densities are compared with those in FEM in Figures 8 through 13. For the sake of good judgment, similar mesh constructions are used for both of the FE and EMCN methods. As it is observed from the figures, the proposed method has accurately modeled the electromagnetic brake with moving solid conductor in all regions and at all speeds. The maximum discrepancy is less than 3%. In the proposed method, by taking into account the primary knowledge of magnetic flux paths, the complexity of the problem can be reduced considerably, without sensible loss of accuracy of the results.

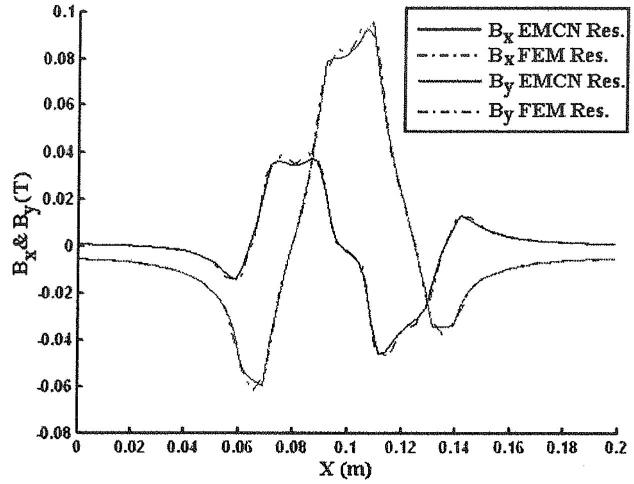

Figure 8: Magnetic flux density in the middle of the air gap at $Vx = 2$ m/s.

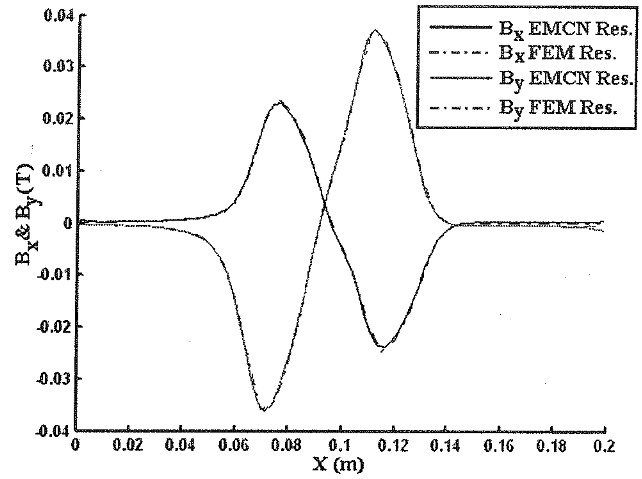

Figure 11: Magnetic flux density in the middle of the moving part at $Vx = 20$ m/s.

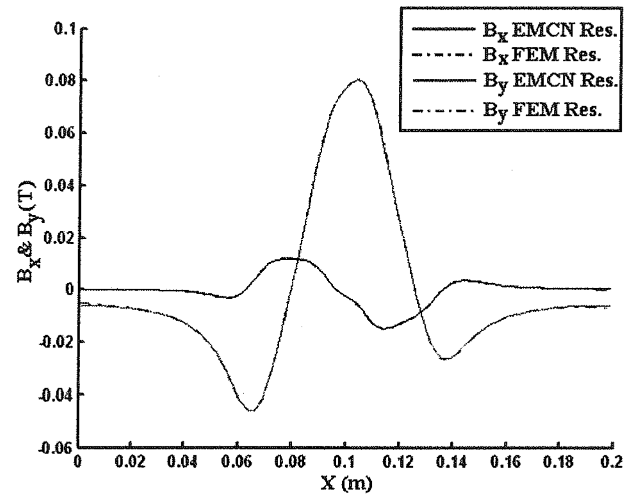

Figure 9: Magnetic flux density in the middle of the moving part at $Vx = 2$ m/s.

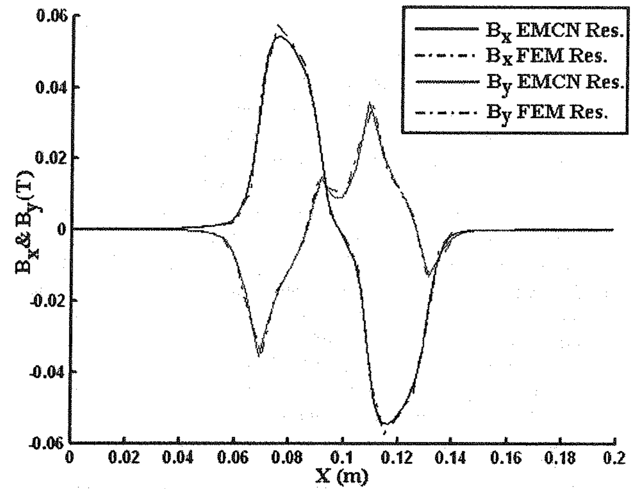

Figure 12: Magnetic flux density in the middle of the air gap at $Vx = 50$ m/s.

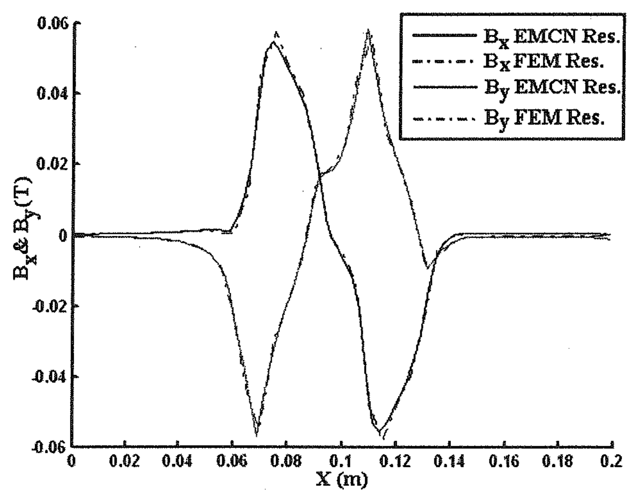

Figure 10: Magnetic flux density in the middle of the air gap at $Vx = 20$ m/s.

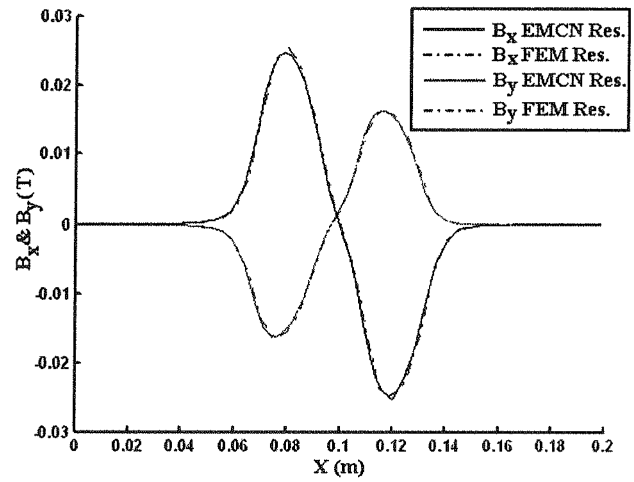

Figure 13: Magnetic flux density in the middle of the moving part at $Vx = 50$ m/s.

4. Conclusion

In this paper a new formulation of magnetic equivalent circuit method has been developed for modeling motional eddy current problems. The proposed method is efficient in processor time and memory storage requirements. Comparison of simulation results with those of the FEM proves the accuracy of the developed method.

5. References

[1] H. Gholizad, M. Mirsalim, M. Mirzayee and I. A. Tsukerman, "Motional eddy current analysis in moving solid iron using magnetic equivalent circuits method," in *Proc. IEEE/ACES International Conference on Wireless Communications and Applied Computational Electromagnetics,* April 3-7, 2005, pp. 533 - 536

[2] V. Ostovic, *Dynamics of Saturated Electric Machines,* New York: Springer-Verlag, 1989.

[3] J. Perho, "Reluctance network for analyzing induction machines," Ph.D. Dissertation, Dept. Electrical Eng., Helsinki University of Technology, Finland, 2002.

[4] J. Hur, I. S. Jung and D. S. Hyun, "Lateral characteristic analysis of PMLSM considering overhang effect by 3-D equivalent magnetic circuit method," *IEEE Trans. on Magnetics,* vol. 34, no. 5, pp. 3142-3145, Sep. 1998.

[5] J. Davidson and M. Balchin, "Three dimensional eddy current calculation using a network method," *IEEE Transactions on Magnetics*, vol. 19, no 6, pp. 2325 – 2328, Nov. 1983.

[6] C. Delforge and B. L. Semail, "Induction machine modeling using finite element and permeance network methods," *IEEE Trans. on Magnetics*, vol. 31, no. 3, pp. 2092-2095, May 1995.

[7] Jin Hur, Hamid. A. Toliyat and Jung-Pyo Hong, "Dynamic analysis of linear induction motors using 3-D equivalent magnetic circuit network (EMCN) method," *Electric Power Components and Systems,* vol. 29, pp. 531-541, 2001.

[8] J. Hur, D. S. Hyun and S. S. Kim, "Three dimensional eddy current calculation using magnetic scalar potential in conducting regions," *Journal of Applied Physics*, vol. 3, no 10, pp. 8314-8316, May 2002.

[9] J. Hur, H. A. Toliyat and J. Hong, "3-D time-stepping analysis of induction motor by new equivalent magnetic circuit network method," *IEEE Trans. on Magnetics*, vol. 37, no. 5, pp. 3225-3228, Sept. 2001.